Dark Matter

ASTR 333/433
Spring 2024
TR 11:30am–12:45pm
Sears 552

http://astroweb.case.edu/ssm/ASTR333/

Prof. Stacy McGaugh
Sears 558
368-1808
stacy.mcgaugh@case.edu

Case Western Reserve
University
Est. 1826

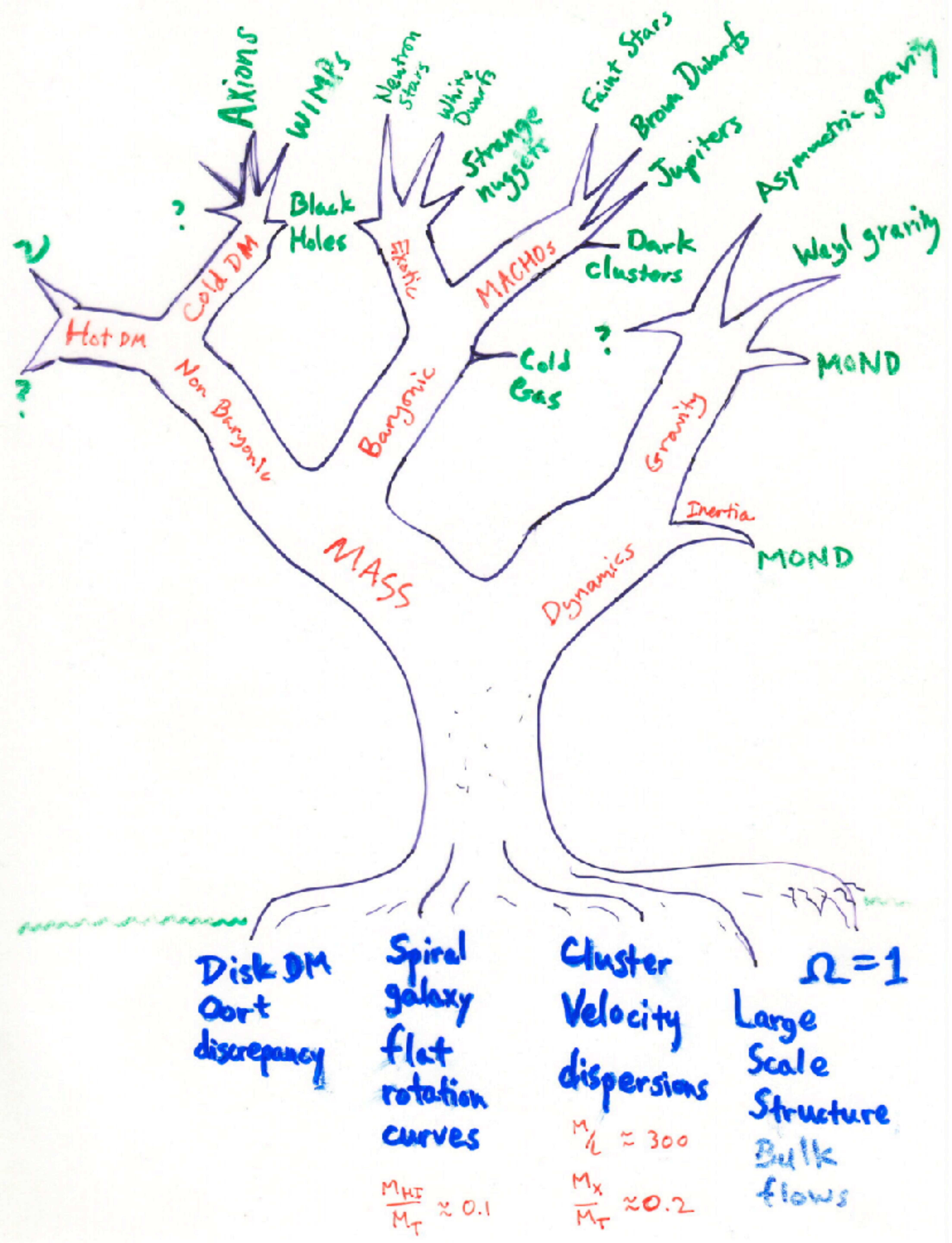

Empirical Laws of Galactic Rotation

- Flat rotation curves (Rubin-Bosma Law)

  Rotation curves tend asymptotically towards a constant rotation velocity that persists to indefinitely large radii: $V(R \to \infty) \to V_f$

- Tully-Fisher relation (Luminous, Stellar Mass, and Baryonic TF relations)

  The baryonic mass of galaxies scales as the fourth power of the flat rotation velocity: $M_b = AV_f^4$

- Central density relation (lower surface brightness galaxies exhibit larger mass discrepancies)

  The central dynamical surface densities of galaxies is related to their central surface brightnesses: $\Sigma_{dyn}(R \to 0) = f[\Sigma_*(R \to 0)]$

- Renzo's rule (Sancisi's Law)

  "For any feature in the luminosity profile there is a corresponding feature in the rotation curve and vice versa." (Sancisi 2004).

- Radial acceleration relation

  The observed centripetal acceleration is related to that predicted by the observed distribution of baryons: $\mathrm{g_{obs}} = \mathcal{F}(\mathrm{g_{bar}})$

These systematic properties involve a critical acceleration scale.

- Baryonic Tully-Fisher Relation

$$\mathrm{g}_{\dagger}^{\mathrm{BTFR}} = 1.24 \pm 0.14 \times 10^{-10}\ \mathrm{m\,s^{-2}}$$

(McGaugh 2011)

- Central Density Relation

$$\mathrm{g}_{\dagger}^{\mathrm{CDR}} = G\Sigma_{\dagger} = 1.27 \pm 0.05 \times 10^{-10}\ \mathrm{m\,s^{-2}}$$

(Lelli et al. 2016)

- Radial Acceleration Relation

$$\mathrm{g}_{\dagger}^{\mathrm{RAR}} = 1.20 \pm 0.02 \times 10^{-10}\ \mathrm{m\,s^{-2}}$$

(McGaugh et al. 2016)

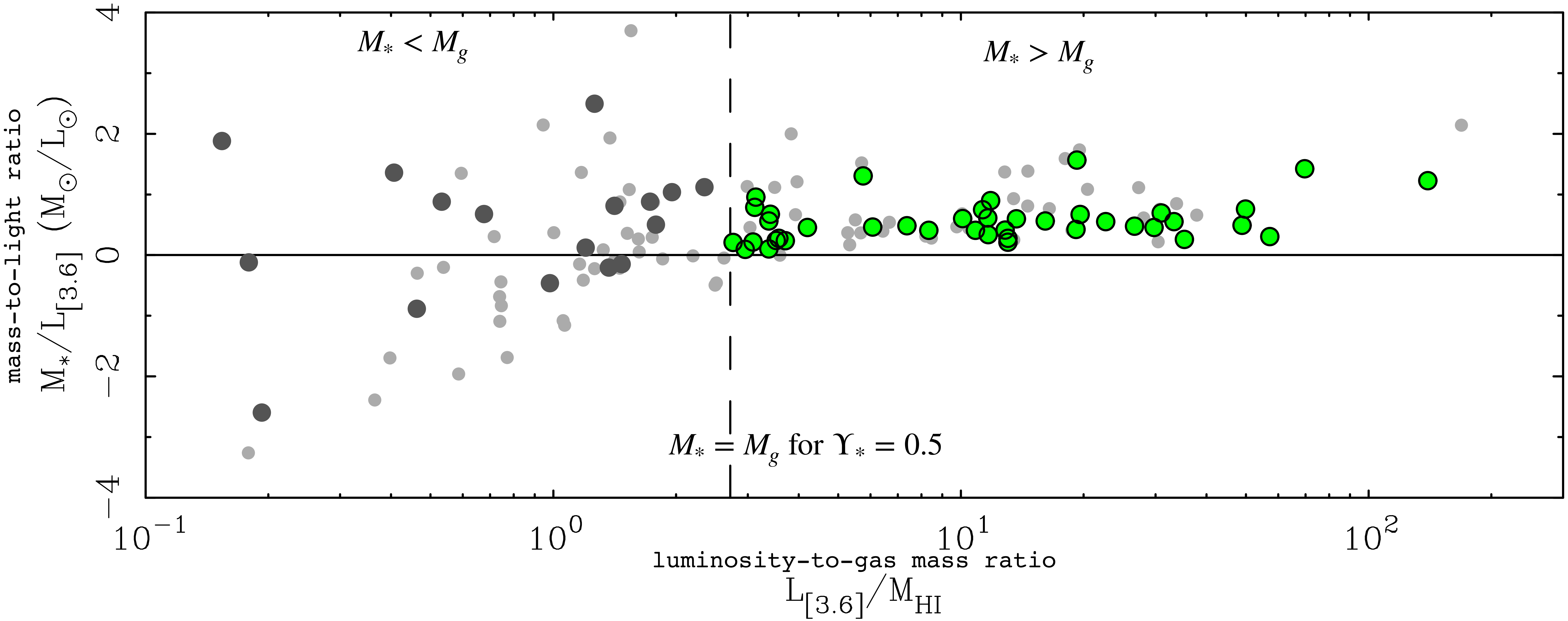

Mass-to-light ratio from BTFR:

$$M_b = M_* + M_g = AV_f^4$$

$$M_* = AV_f^4 - M_g$$

$$\Upsilon_* = (AV_f^4 - M_g)/L$$

Elliptical Galaxies

Elliptical galaxies are presumed to reside in dark matter halos, but the evidence is less obvious than for spirals.

Elliptical Galaxies

composed mostly of older stars

Generic Star Formation History

Elliptical

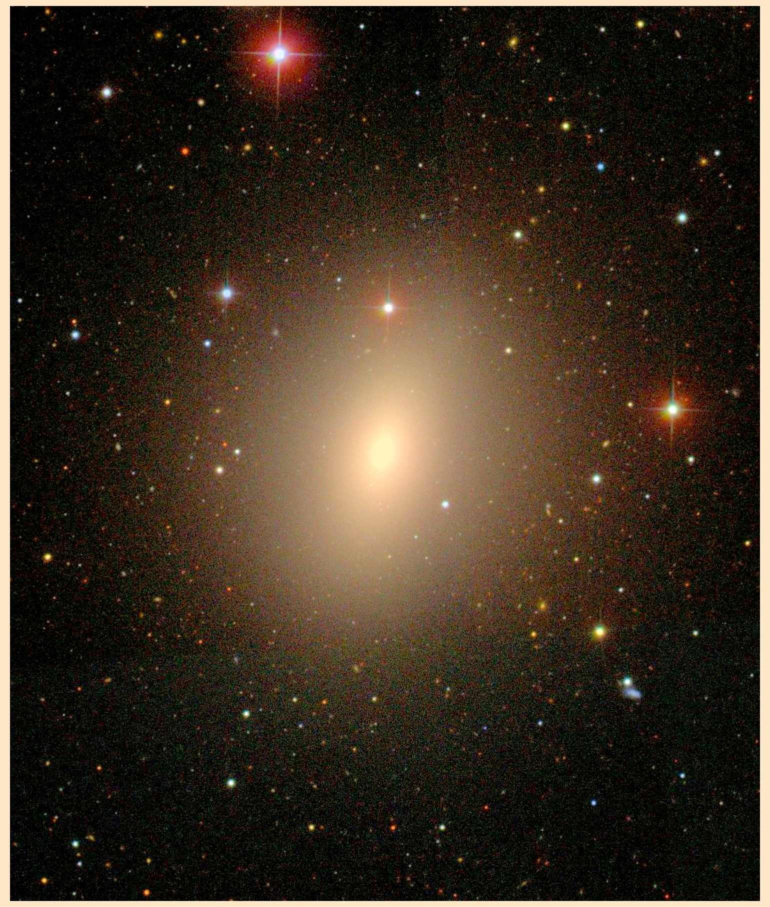

old stars

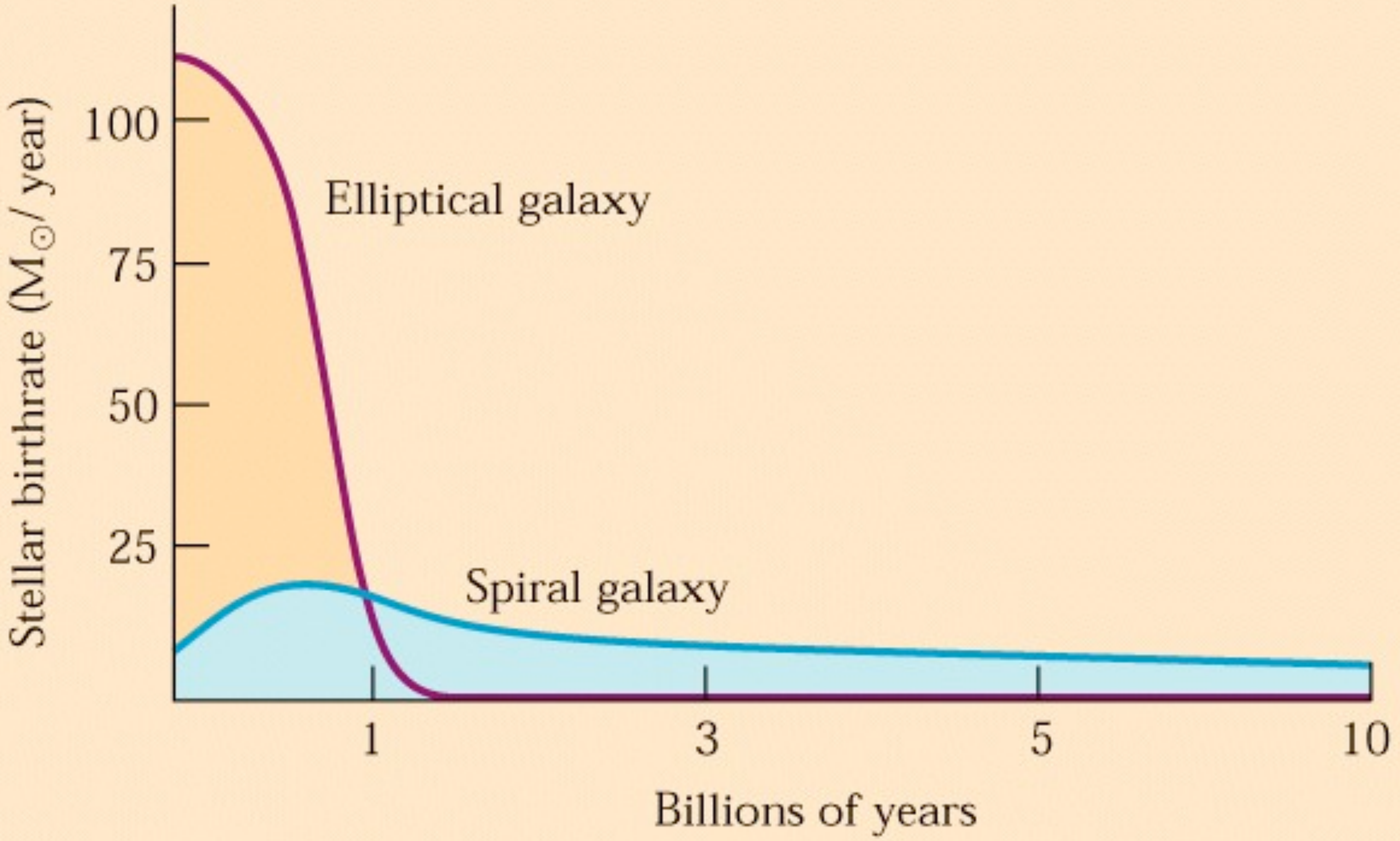

Spiral

old stars
young stars
cold gas

Expect the older stars in elliptical galaxies to have higher mass-to-light ratios than in spirals.

color-magnitude relation for galaxies

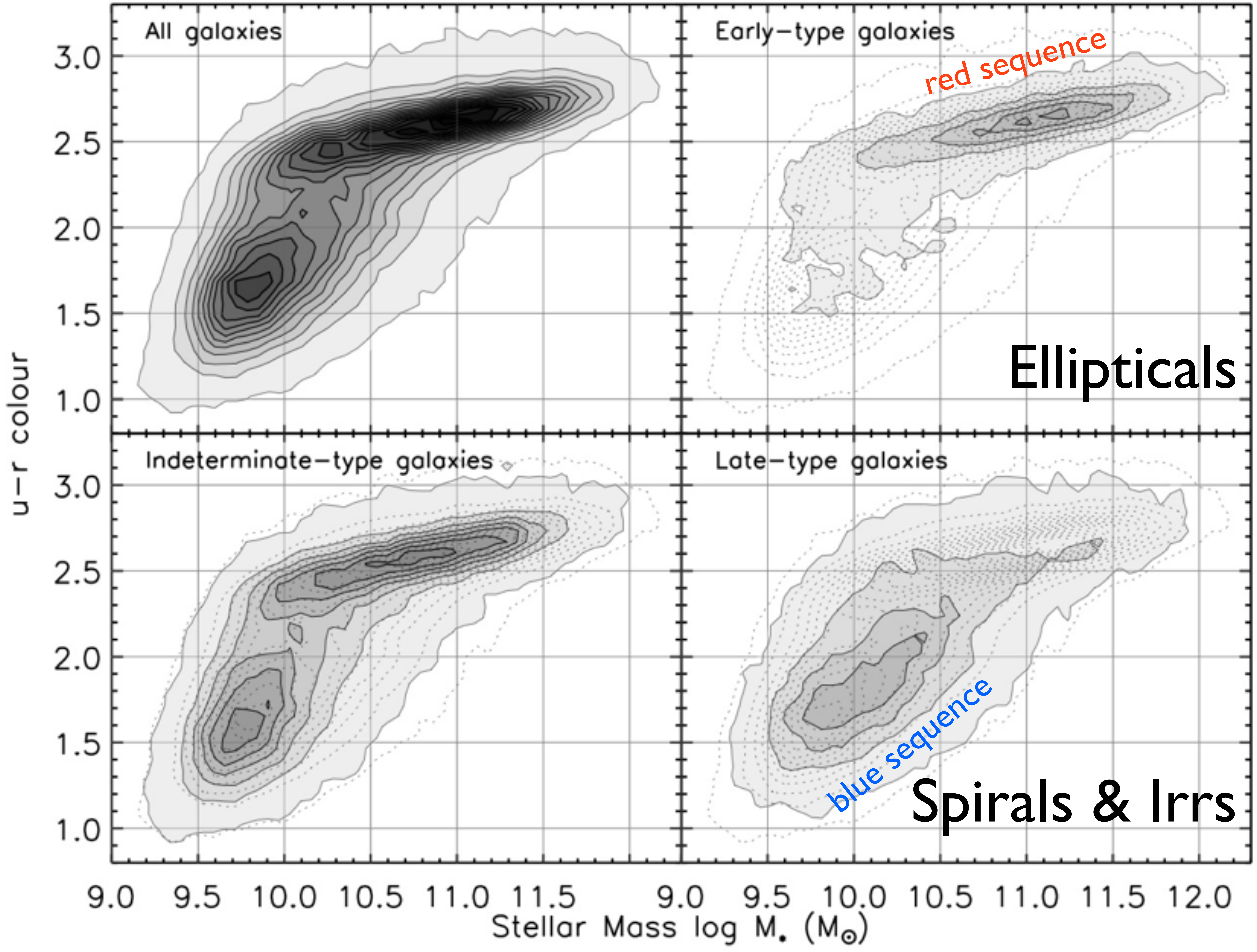

"Main Sequence of Star Forming Galaxies"

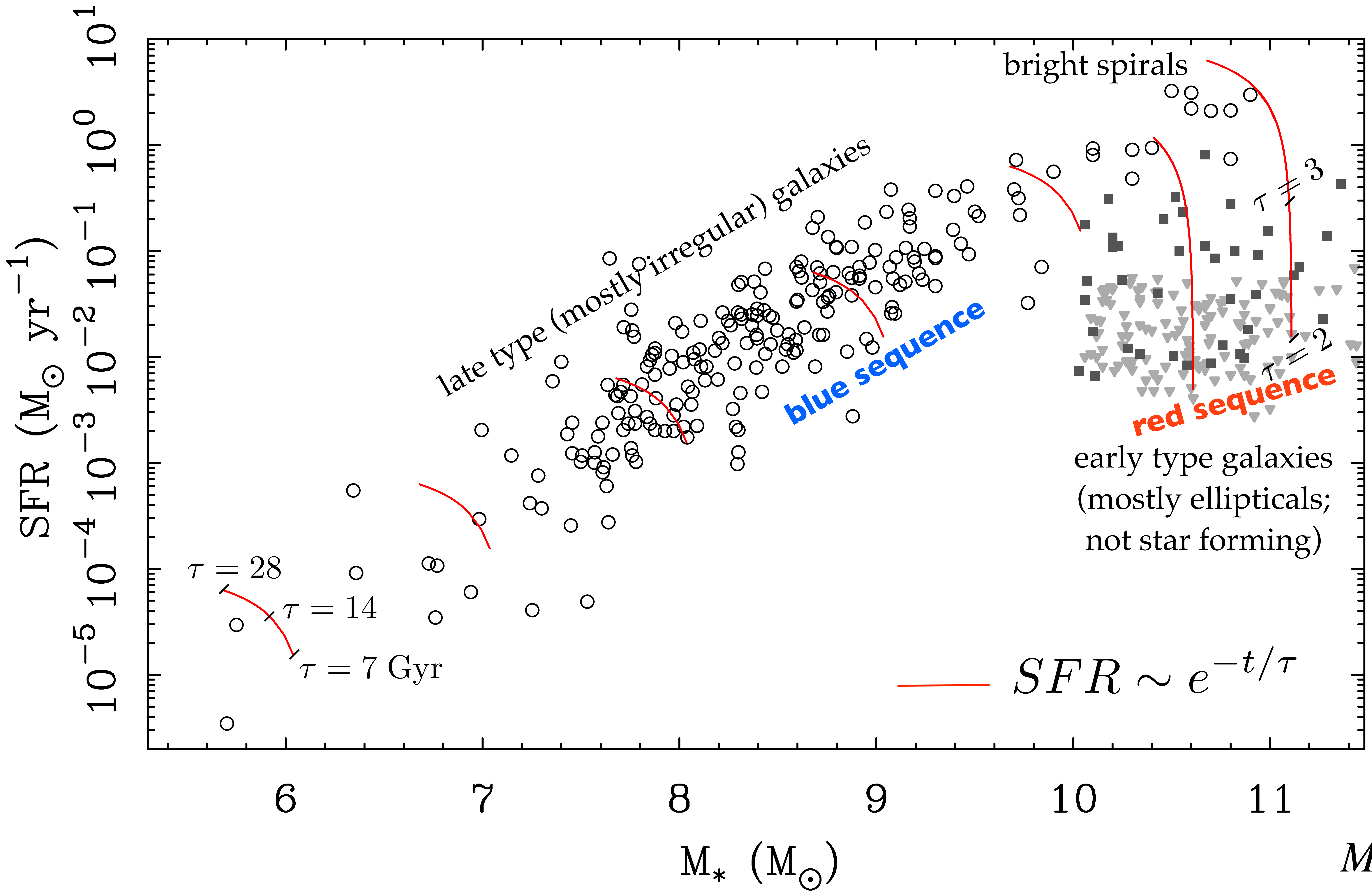

$$M_* = \int SFR\, dt$$

Stellar orbits in galaxies

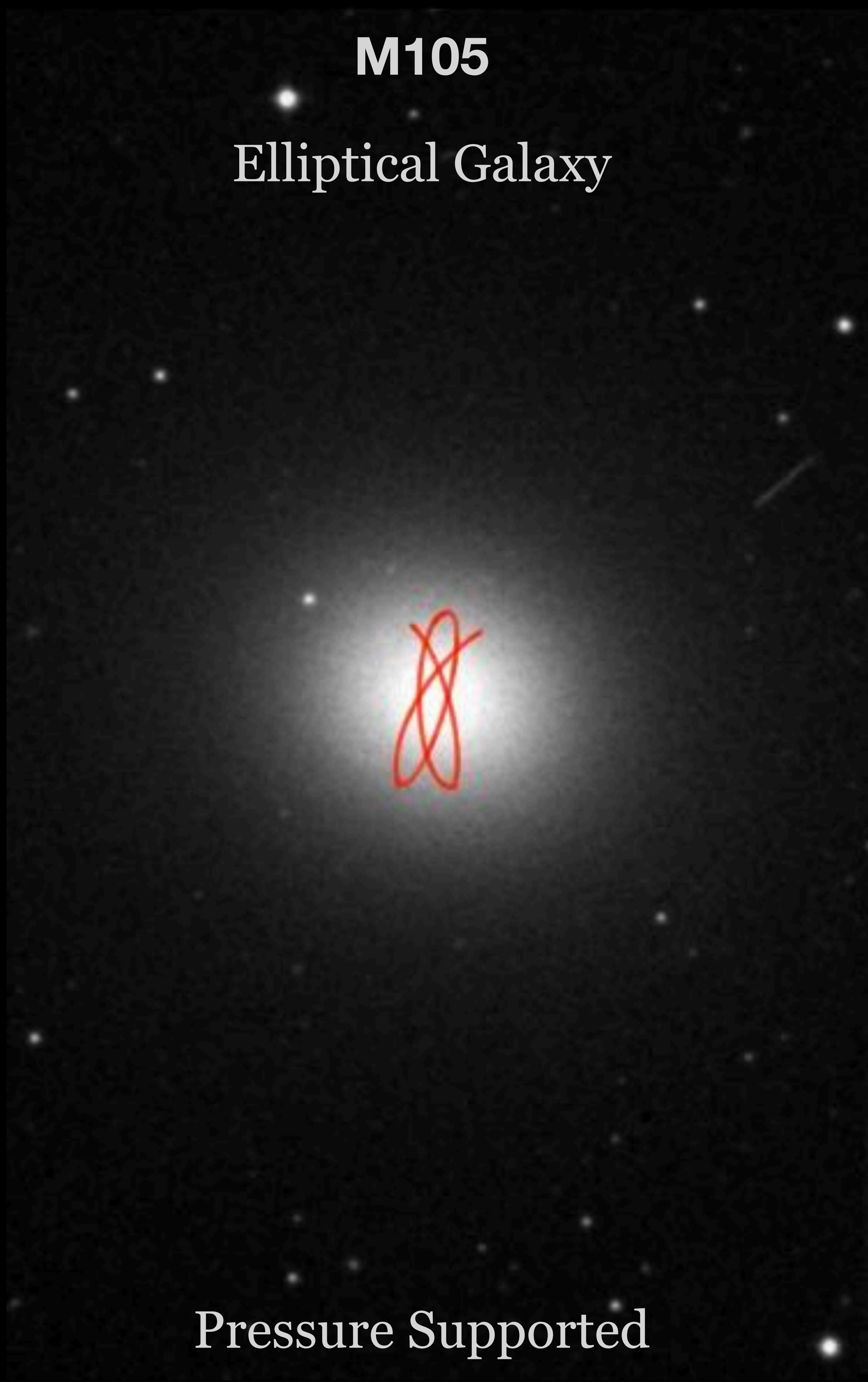

Eccentric radial orbits
Random orientations

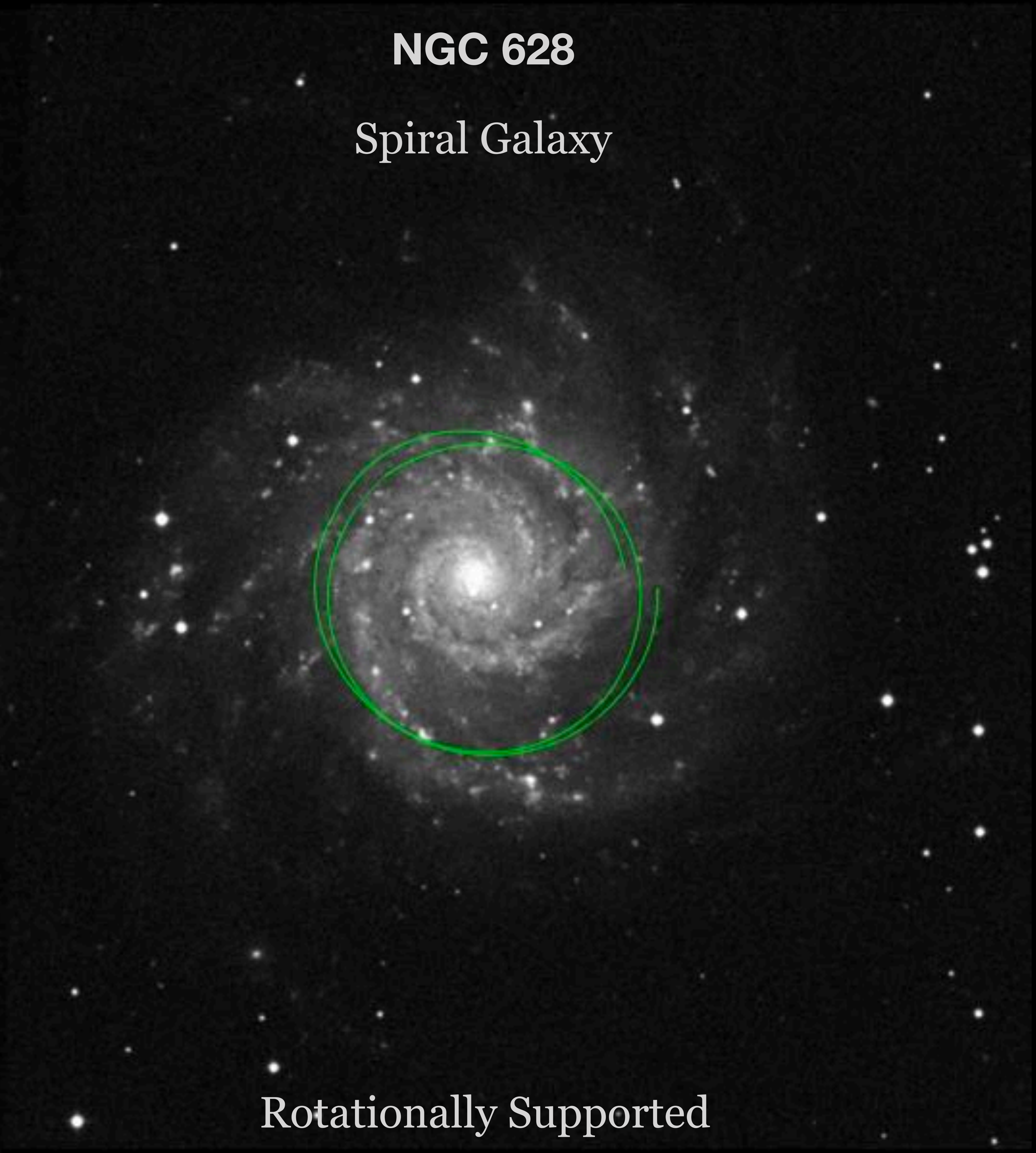

Nearly circular orbits
Same direction, same plane

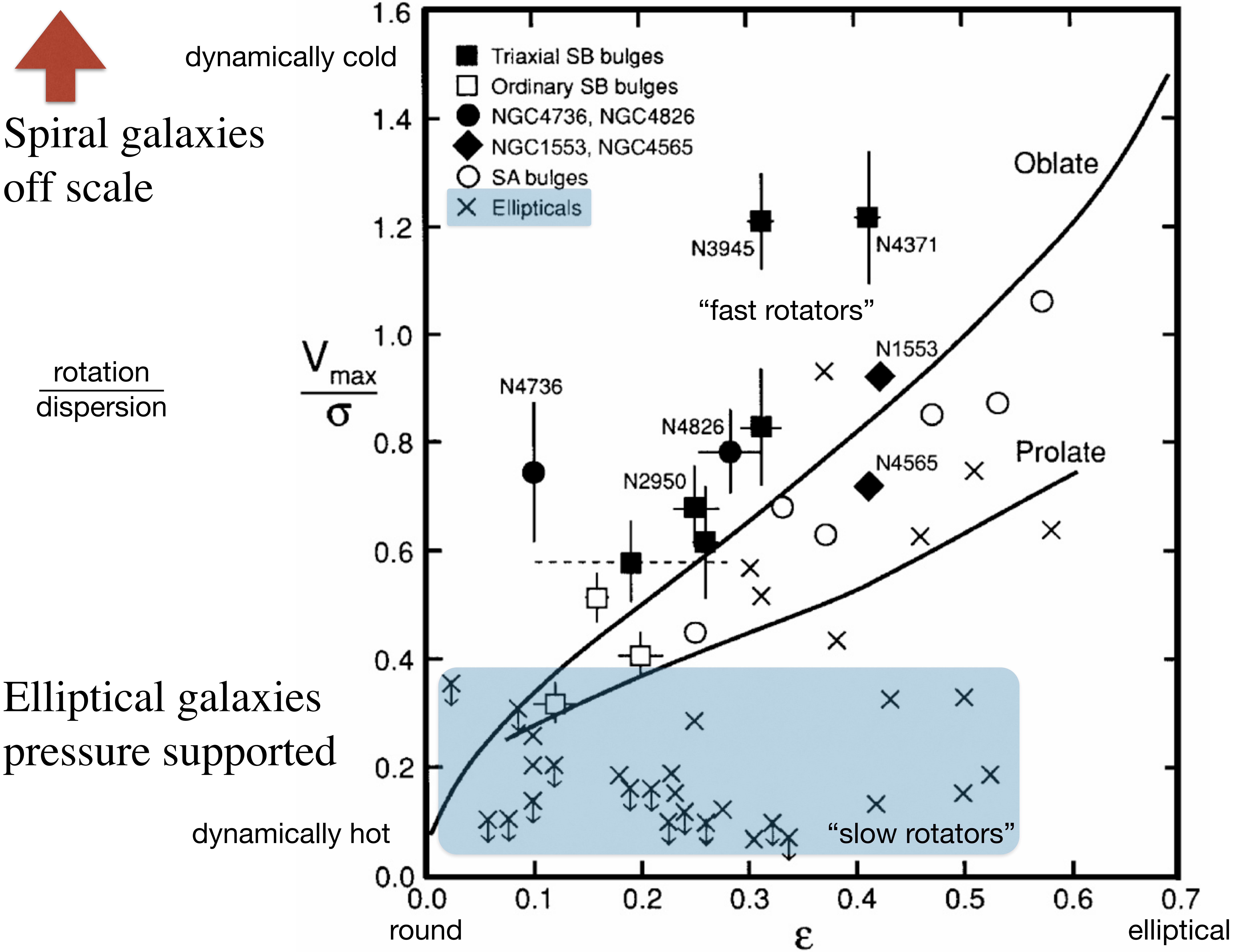

dynamically cold
Spiral galaxies
off scale
rotation
dispersion
V_{max} / σ
Elliptical galaxies
pressure supported
dynamically hot
Triaxial SB bulges
Ordinary SB bulges
NGC4736, NGC4826
NGC1553, NGC4565
SA bulges
Ellipticals
Oblate
Prolate
N3945
N4371
"fast rotators"
N1553
N4736
N4826
N4565
N2950
"slow rotators"
1.6
1.4
1.2
1.0
0.8
0.6
0.4
0.2
0.0
0.0
0.1
0.2
0.3
0.4
0.5
0.6
0.7
round
ε
elliptical

$$\lambda_R = \frac{\langle R|V|\rangle}{\langle R\sqrt{V^2+\sigma^2}\rangle}$$

specific angular momentum

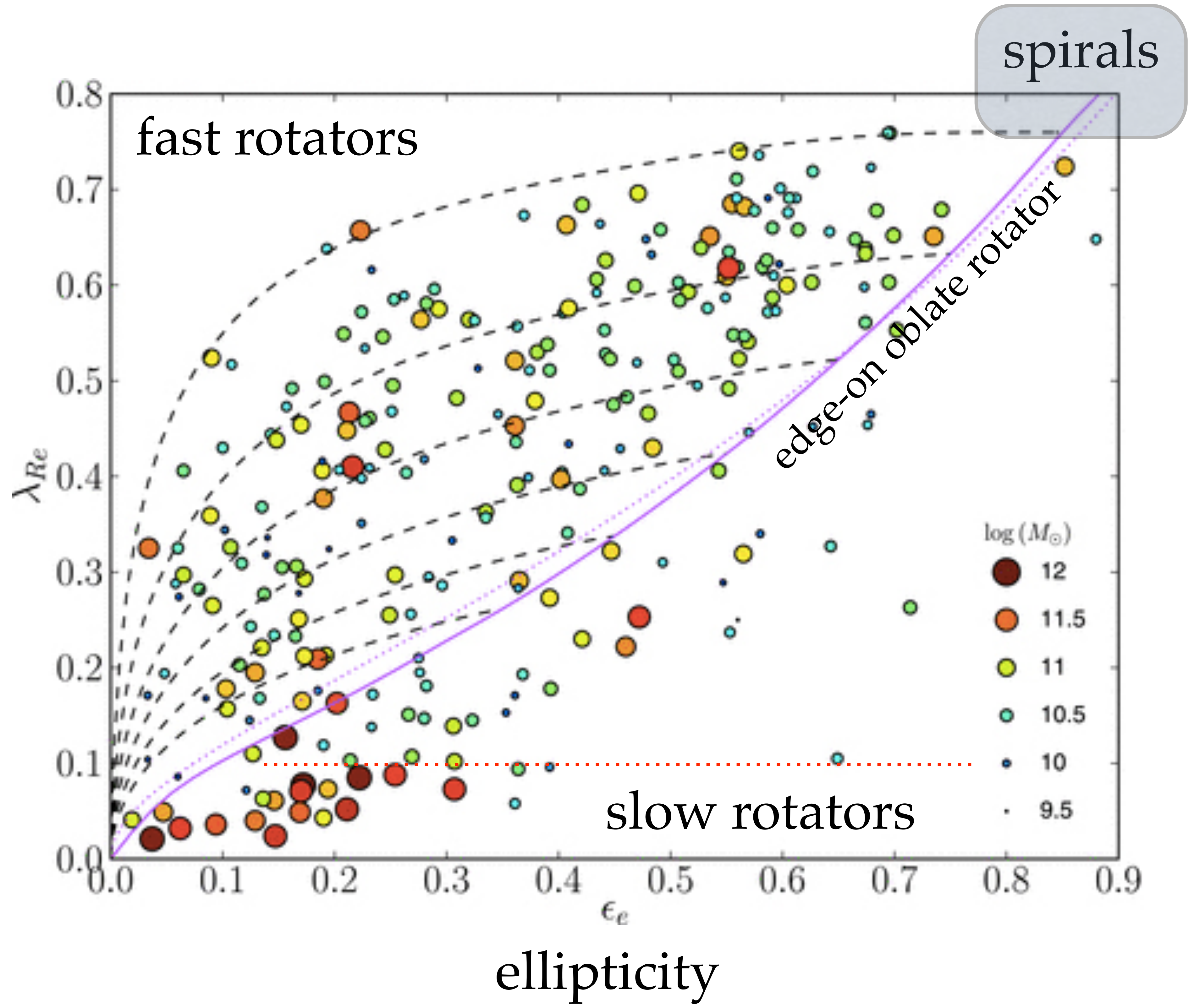

Massive ellipticals mostly pressure supported (slow rotators) while many (not all) lower mass ellipticals are fast rotators. These are often S0 galaxies.

Dashed lines represent different inclinations for different intrinsic ellipticities

Schwarzschild's method

Combine possible orbit families
to best match the data

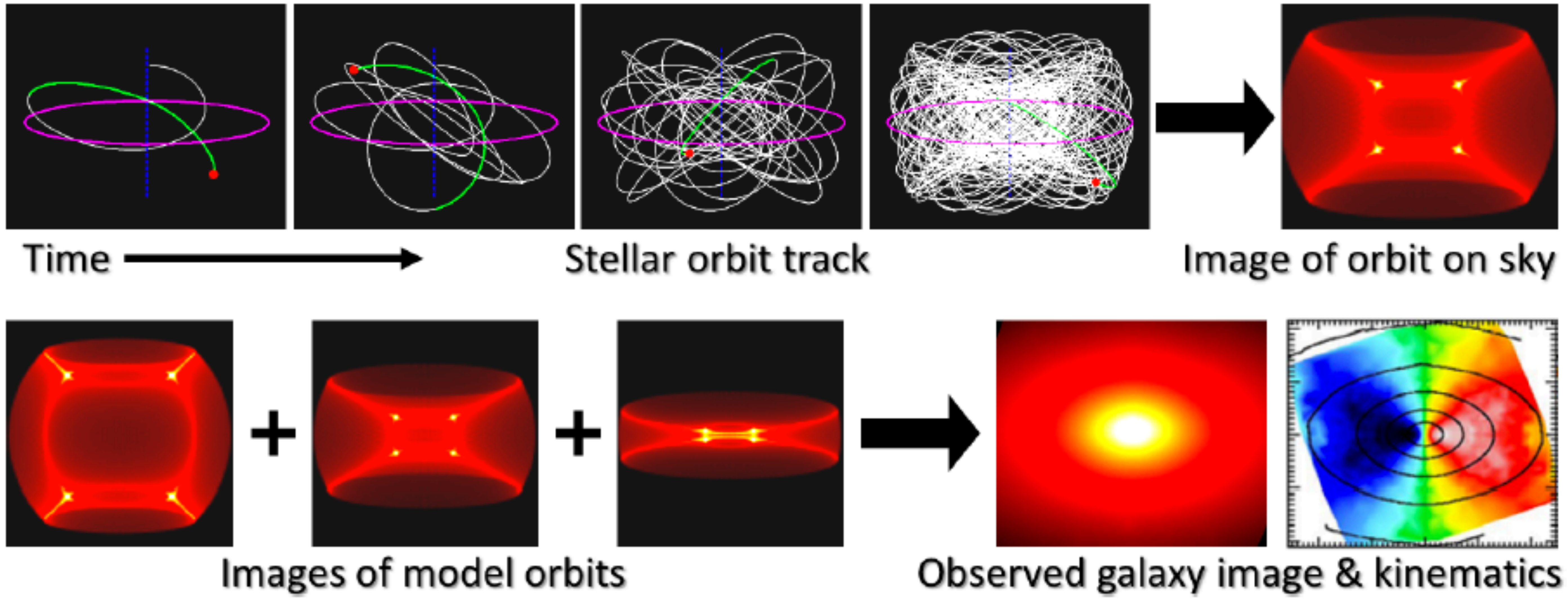

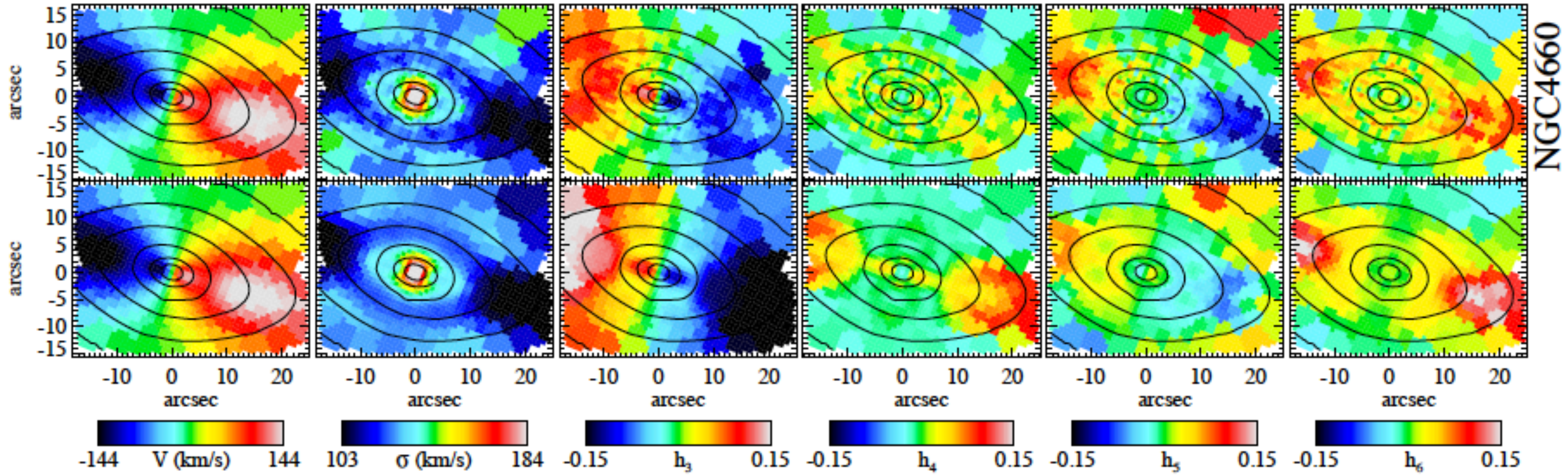

Figure 3. Schwarzschild's orbit-superposition method. *Top Row:* numerical integration of a single orbit in the adopted gravitational potential. After a sufficiently long time the density (of regular orbits) converges to a fixed distribution. *Middle Row:* the method finds the linear combination of thousands of orbits (three representative are shown here) which best fits the galaxy image and stellar kinematics. *Bottom two rows:* data (top) versus model (bottom) comparison. The model can fit the full stellar line-of-sight velocity distribution, here parametrized by the first six Gauss-Hermite moments (from Cappellari et al. 2007).

anisotropy

Orbital Anisotropy

The anisotropy parameter measures how radial or circular orbits are

anisotropy $$\beta = 1 - \frac{\sigma_t^2}{\sigma_r^2}$$

σ_t^2 ← tangential velocity dispersion

σ_r^2 ← radial velocity dispersion

Jean's equation (one form)

$$GM(r) = r\sigma_r^2\left(-\frac{\partial \ln \nu_*}{\partial r} - \frac{\partial \ln \sigma_r^2}{\partial r} - 2\beta\right)$$

↑ logarithmic gradients (just the power law slope!)

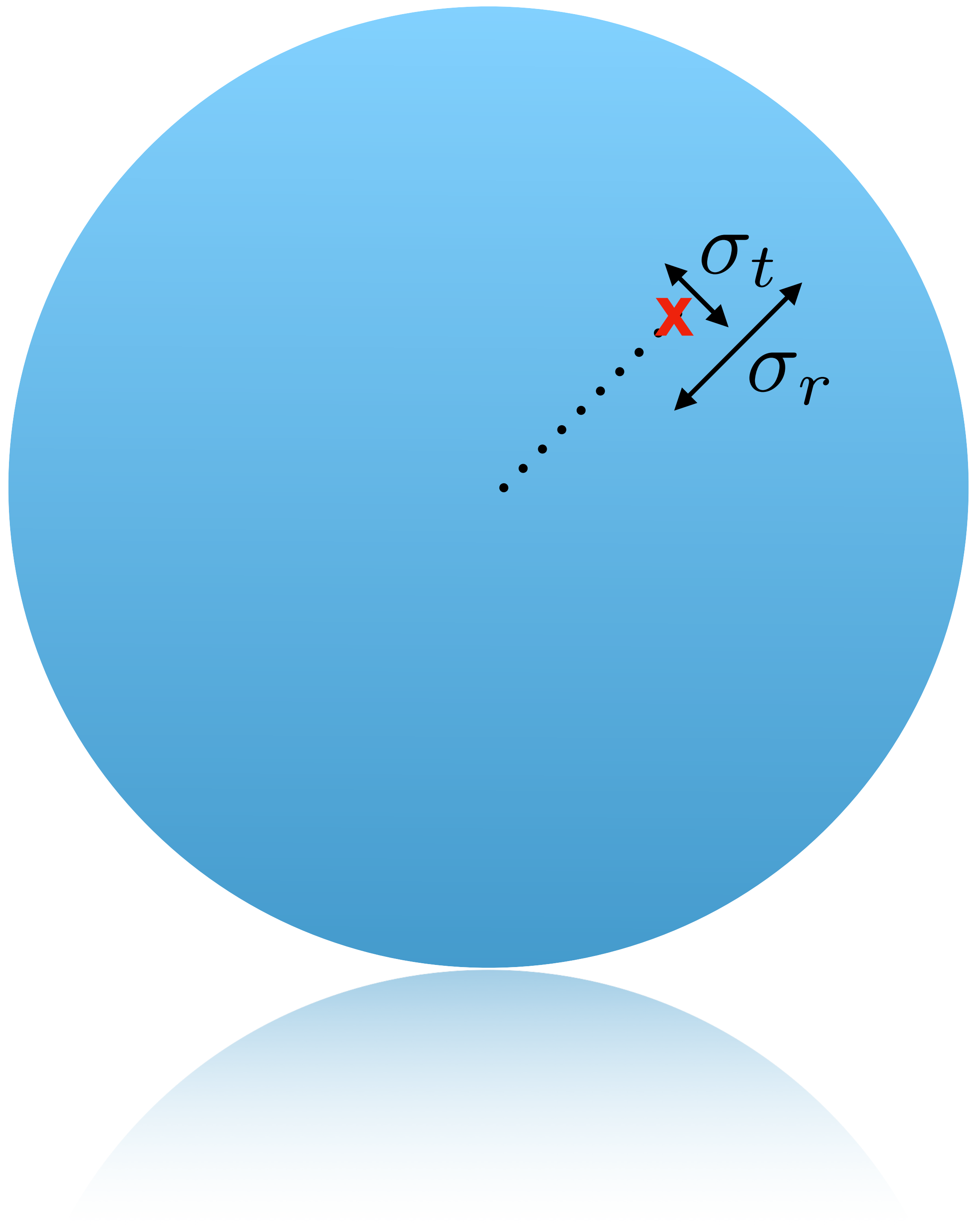

$\nu_*(r)$ is the density distribution of tracer particles
e.g., exponential disk, $r^{1/4}$ law

Phase Space

More generally, can define a combination of configuration and momentum as 6D phase space

phase space $f(x_i, \dot{x}_i)$ configuration space $x_i = x, y, z$ momentum space $\dot{x}_i = \dot{x}, \dot{y}, \dot{z}$

Collisionless Boltzmann equation

$$\frac{\partial f}{\partial t} + \overrightarrow{V} \cdot \overrightarrow{\nabla} f - \overrightarrow{\nabla} \Phi \frac{\partial f}{\partial \overrightarrow{V}} = 0$$

Works for equilibrium systems; relying on the fact that the gravitational potential depends only on position, not momentum.

PHASE SPACE IS CONSERVED
Can mix in empty space (spread things out), but cannot compress.

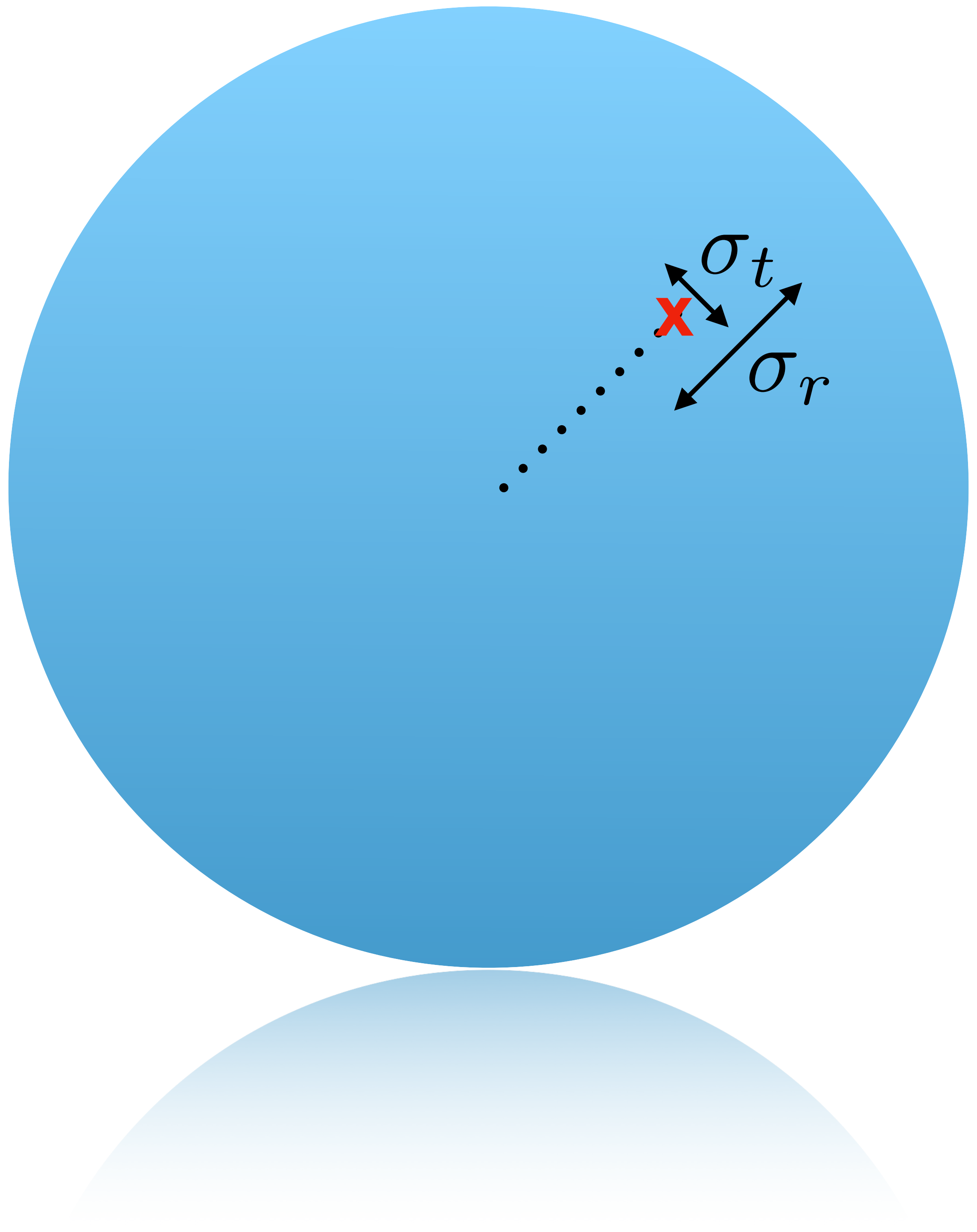

Fornax

dwarf spheroidal (dSph)
satellite of the Milky Way

Jean's equation $GM(r) = r\sigma_r^2 \left(-\frac{\partial \ln \nu_*}{\partial r} - \frac{\partial \ln \sigma_r^2}{\partial r} - 2\beta \right)$

Mass-anisotropy degeneracy

$M(r)$ degenerate with $\beta(r)$

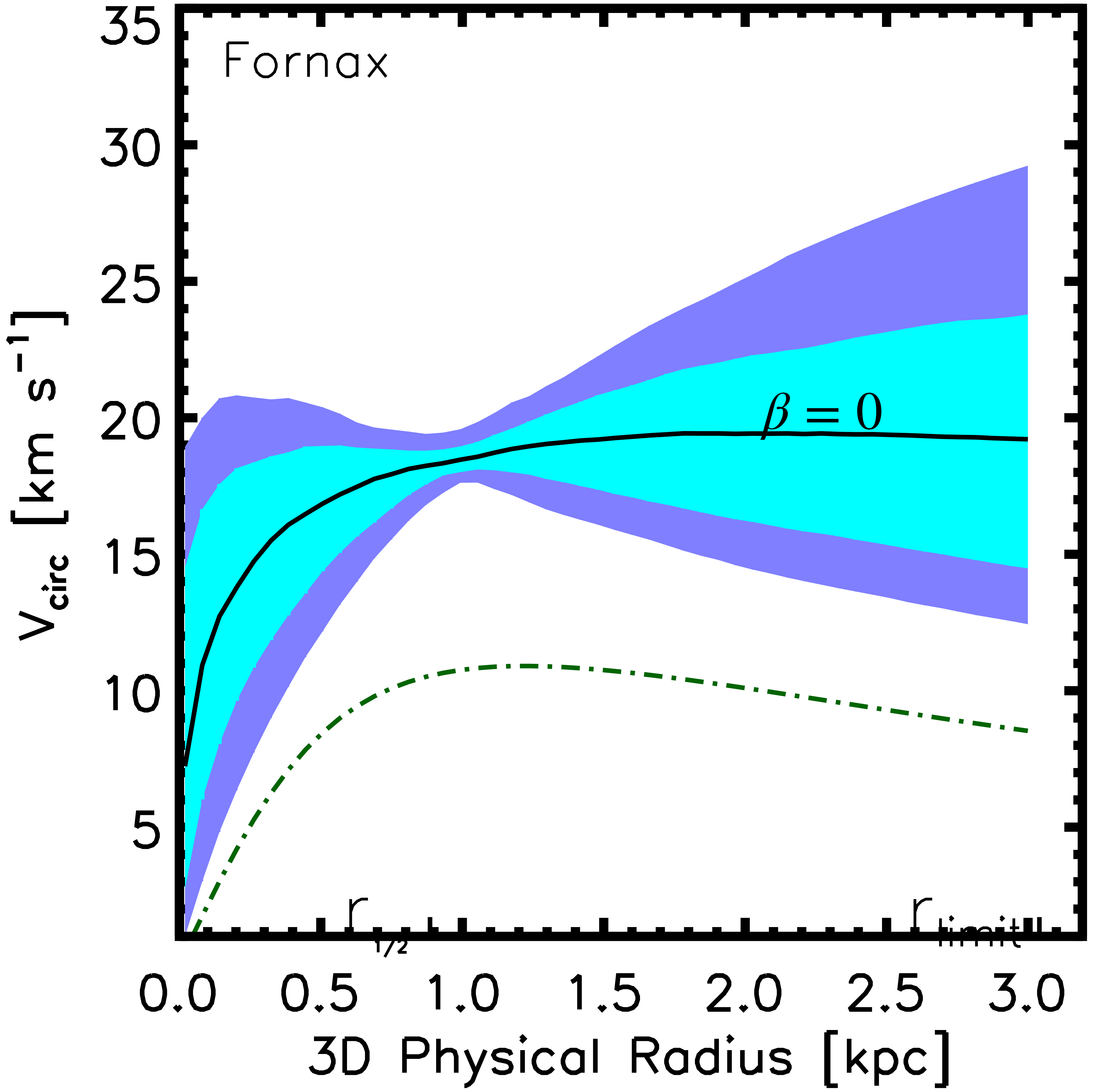

Velocity dispersion profiles for 3 ETGs
measured from stars at small R, PN at large R

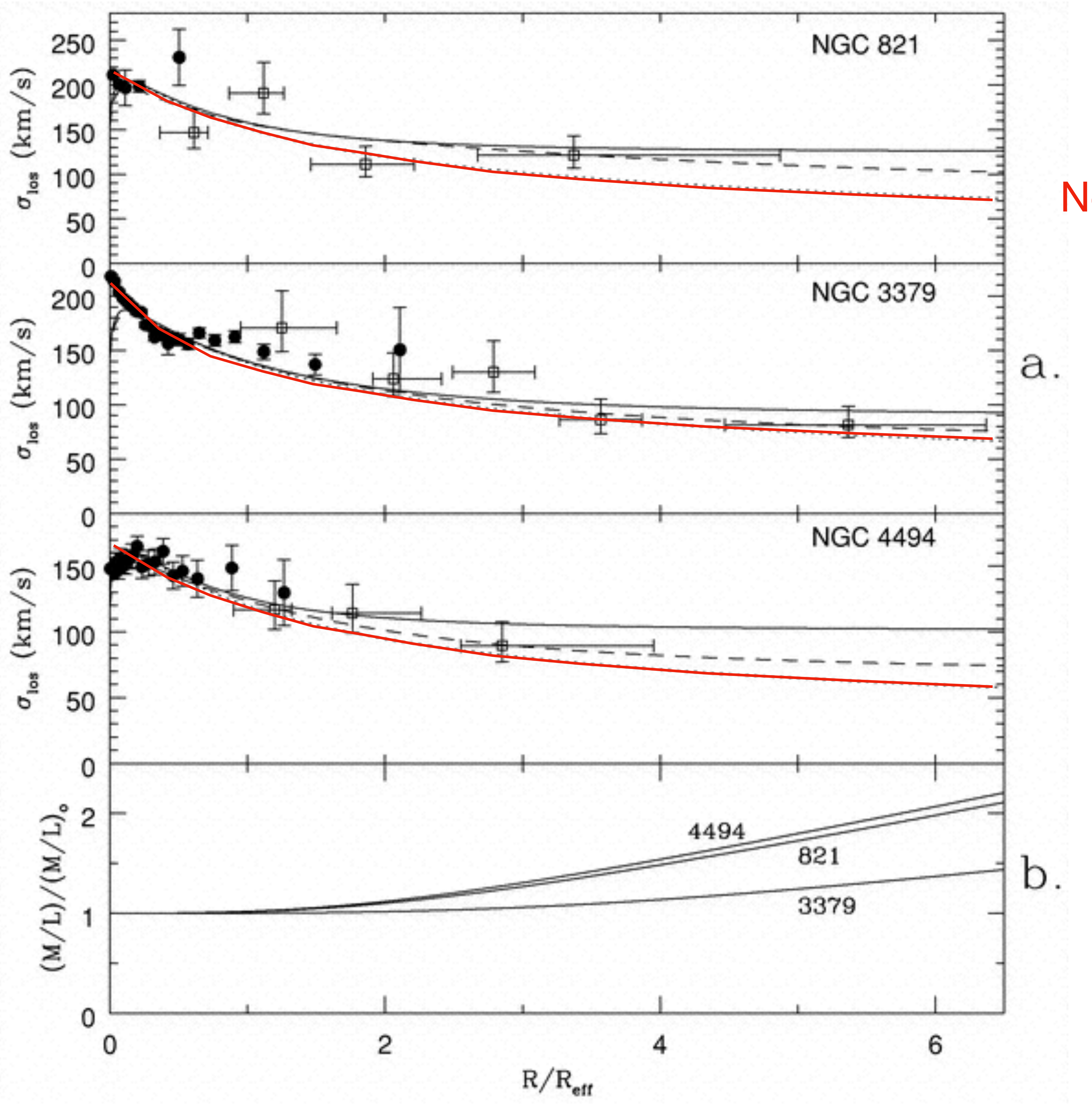

No dark matter

Radial Acceleration Relation in Elliptical galaxies

ATLAS^{3D} data (fast rotators)

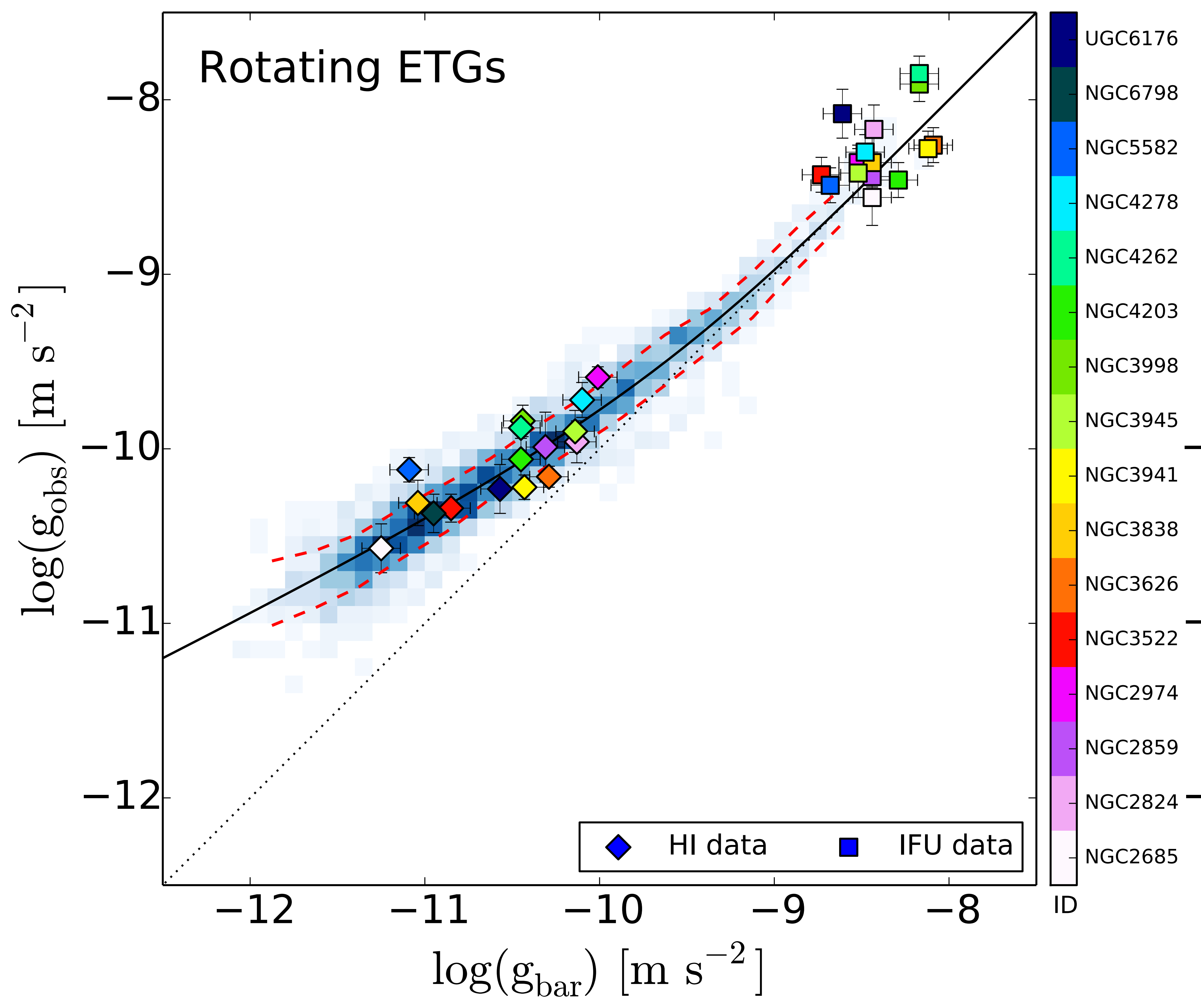

Inner, high acceleration data from optical IFU
Outer, low acceleration points from HI 21 cm

X-ray Ellipticals (slow rotators)

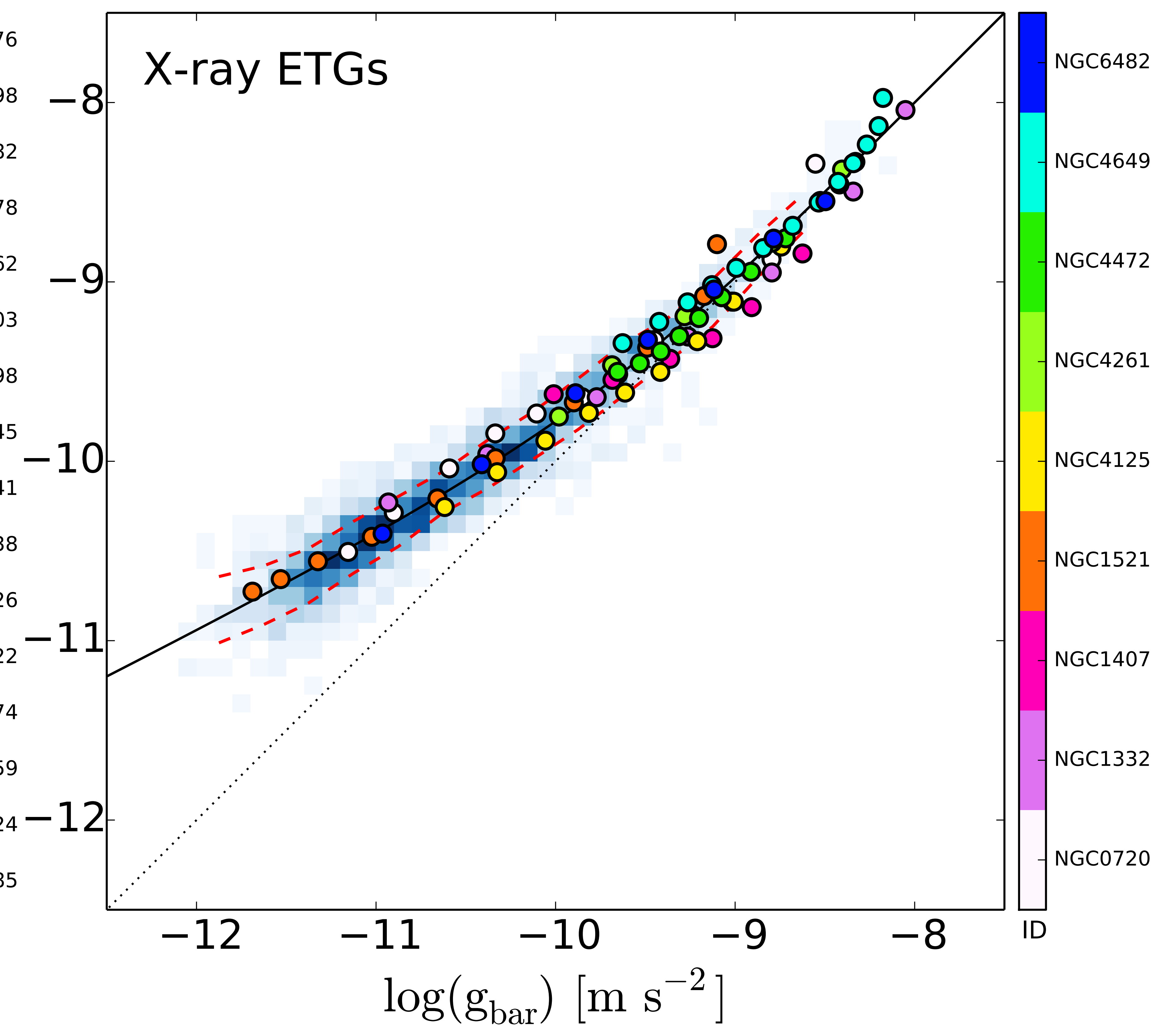

Mass profiles from hydrostatic equilibrium of X-ray gas.